Supporting Information

Chang et al. 10.1073/pnas.0912969107

SI Text

Electrodynamic Calculation of Forces on Dielectric Sphere. Here we describe in detail the point-dipole approximation for a sub-wavelength dielectric sphere, and compare the results of this approximation with exact numerical electrodynamic calculations of the optical forces. For concreteness, we consider a dielectric sphere of (possibly complex) permittivity ϵ and radius r, interacting with an incident standing electromagnetic wave with electric and magnetic field components $\mathbf{E}_{\text{in}} = \hat{y}E_0 \cos k(x - x_0) \cos \omega t$ and $\mathbf{B}_{\text{in}} = \hat{z}(E_0/c) \sin k(x - x_0) \sin \omega t$, where $k = \omega/c$. Here we assume that the sphere is in free space rather than in a cavity, which allows one to unambiguously calculate the optical forces acting on the sphere independent of its motion (as opposed to the cavity case where the motion of the sphere generally shifts the cavity resonance, causing the intracavity field $E_0(t)$ to depend on the history of motion). In the special case where the sphere is localized near one of the nodes or anti-nodes, the free-space and cavity cases yield the same results (e.g., for the mechanical trap frequency ω_m) as the cavity resonance and intra-cavity field to lowest order become insensitive to small displacements of the sphere. The electrodynamic problem of plane-wave scattering off of a sphere is exactly solvable, as the vector wave equation $\nabla^2\mathbf{E}(\mathbf{r}) + k^2\epsilon(\mathbf{r})\mathbf{E}(\mathbf{r}) = 0$ (with similar equation for $\mathbf{B}$) admits solutions through separation of variables (1). Note that one can define natural dimensionless length scales $k|\sqrt{\epsilon}|r$, kr for the electrodynamic response inside and outside the sphere. Of particular interest is the case when $k|\sqrt{\epsilon}|r \ll 1$ is a small parameter (we assume that $|\sqrt{\epsilon}| > 1$ for this discussion, which is typically the case). One can then formally solve the wave equations using perturbation theory, with the lowest order equation given by $\nabla^2\mathbf{E}(\mathbf{r}) = 0$ along with appropriate boundary conditions at the surface of the sphere. Physically, this approximation states that the magnetic field is not important in the near-field, such that the lowest-order response of the sphere can be obtained by solving an electrostatic equation. Taking an optical wavelength of $\lambda = 2\pi/k = 1\,\mu\text{m}$ and $\epsilon = 2$, for instance, the electrostatic solution should be valid for $r \lesssim 110$ nm. In this regime, the polarizablity of the sphere is of the simple form given by electrostatic theory, $\alpha_{\text{ind}} = 3\epsilon_0 V \frac{\epsilon-1}{\epsilon+2}$ (1), as is used in the main text. The optical potential experienced by the sphere is predicted to be $U_{\text{opt}} = -(1/4)(\text{Re}\,\alpha_{\text{ind}})E_0^2 \cos^2 k(x - x_0)$. For spheres larger than $r \gtrsim 1/k|\sqrt{\epsilon}|$, the forces predicted by the electrostatic theory will be substantially larger than the actual forces, as phase variations of the field within the sphere become important.

To compare the electrostatic approximation with actual results, we first solve the electrodynamic scattering problem exactly. The exact force F_x along x can then be obtained by integrating the Maxwell stress tensor T_{ij} over the sphere surface S,

$$F_x = \epsilon_0 \oint_S da \sum_{j=x,y,z} T_{xj}\hat{n}_j, \qquad \text{[S1]}$$

where $\hat{n}_j$ is the outgoing normal vector to the sphere surface. In Fig. S1 we compare the approximate and exact forces for various values of r, taking $\epsilon = 2$. It can be seen that the two methods agree closely for $k\sqrt{\epsilon}r \lesssim 1$. For spheres where $k\sqrt{\epsilon}r \gtrsim 1$, the forces predicted from electrostatic theory can be much larger than the actual forces, and even different in sign.

Absorption losses of trapped sphere. In this section, we consider the effect that a small imaginary component of the permittivity ϵ has on a trapped sphere. In the limit that the sphere has a radius much smaller than the optical wavelength, the sphere behaves as a point-like dipole with polarizability $\alpha_{\text{ind}} = 3\epsilon_0 V \frac{\epsilon-1}{\epsilon+2}$. For small Im ϵ, the polarizability acquires a small imaginary component that leads to a non-zero absorption cross-section, with a corresponding absorbed power

$$P_{\text{abs}} = 12\pi \frac{I_0}{\lambda} V \text{Im} \frac{\epsilon - 1}{\epsilon + 2}. \qquad \text{[S2]}$$

Here I_0 is the trapping beam intensity, V is the sphere volume, and λ is the optical wavelength. The absorbed power causes a rise in the internal temperature T_{int} of the sphere, which is balanced out by thermalization with a background gas and blackbody radiation.

We first quantify the effect of the background gas (which is negligible in the regime of particular interest where the sphere is trapped under good vacuum conditions). There are two limiting regimes to the background gas interactions, where the sphere radius is either much smaller or larger than the molecular mean free path λ_{mfp}. At a relatively large pressure of $P = 1$ Torr and room temperature, $\lambda_{\text{mfp}} \sim 100\,\mu\text{m}$ and thus our case of interest is always $r \ll \lambda_{\text{mfp}}$. Here, gas molecules independently collide and partially thermalize with the sphere. This leads to a cooling rate (2)

$$\frac{dE}{dt} = -\alpha_g \sqrt{\frac{2}{3\pi}} (\pi r^2) P v_{\text{rms}} \frac{\gamma_{\text{sh}} + 1}{\gamma_{\text{sh}} - 1} \left(\frac{T_{\text{int}}}{T} - 1 \right), \qquad \text{[S3]}$$

where P, v_{rms}, T are the background gas pressure, root-mean-square speed, and temperature, respectively, and γ_{sh} is the gas specific heat ratio ($\gamma_{\text{sh}} = 7/5$ for an ideal diatomic gas). α_g is a phenomenological energy accommodation factor ($0 \le \alpha_g \le 1$), which characterizes the degree to which a gas molecule thermalizes with the sphere upon a single collision.

Under good vacuum conditions, blackbody radiation dissipates the majority of the power absorbed by the sphere. For the submicron spheres we are considering, the radius is much smaller than the absorption length at typical blackbody radiation wavelengths, and thus the usual formulas for blackbody radiated power do not apply. Instead, the sphere again behaves as a point-like dipole at these wavelengths, e.g., the radiated power scales like volume (as opposed to surface area in the case of a large object). The internal heating rate due to blackbody radiation is given by $dE/dt = \sum_{\mathbf{k}} (\hbar ck) R_{\text{abs},\mathbf{k}}$, where the sum is over all blackbody radiation modes (and polarizations), $\mathbf{k}$ is the wavevector of each mode, and $R_{\text{abs},\mathbf{k}}$ is the absorption rate of each mode. It is given by

$$R_{\text{abs},\mathbf{k}} = 3ck(V/V_q) n_k \text{Im} \frac{\epsilon(\omega_k) - 1}{\epsilon(\omega_k) + 2}, \qquad \text{[S4]}$$

where $n_k = (e^{\hbar ck/k_B T} - 1)^{-1}$ is the occupation number of each mode and V_q is the quantization volume. Assuming that the sphere has a relatively constant and temperature-independent permittivity $\epsilon(\omega) \approx \epsilon_{\text{bb}}$ across the blackbody radiation spectrum, it is straightforward to show that the sphere absorbs blackbody radiation at a rate

$$\frac{dE}{dt} = \frac{72\zeta(5)}{\pi^2} \frac{V}{c^3\hbar^4} \text{Im} \frac{\epsilon_{\text{bb}} - 1}{\epsilon_{\text{bb}} + 2} (k_B T)^5, \qquad \text{[S5]}$$

where T is the background temperature and $\zeta(5) \approx 1.04$ is the Riemann zeta function. Similarly, the sphere radiates blackbody energy at a rate given by the negative of Eq. **S5**, with the substitution $T \to T_{\rm int}$.

To illustrate these results, in Fig. S2*A–C* we plot the internal equilibrium temperature $T_{\rm int}$ of the sphere as a function of background gas pressure and trapping intensity I_0. Here we have taken into account the effects of optical absorption (Im ϵ), thermalization with the background gas, and blackbody radiation. The values of Im ϵ in Fig. S2*A–C* correspond to bulk optical absorption rates of $10, 100, 1000$ dB/km, respectively, while the real part of the permittivity is chosen to be Re $\epsilon = 2$. We have taken the other parameters to be $r = 50$ nm, $\alpha_g = 0.25$, Im $\frac{\epsilon_{\rm bb}-1}{\epsilon_{\rm bb}+2} = 0.1$ (roughly corresponding to the averaged value of fused silica around blackbody wavelengths) (3), and a volumetric heat capacity of the sphere of $\tilde{c} = 2{\rm J/m^3 \cdot K}$. Note that at sufficiently low pressures, the temperature becomes pressure-independent as only blackbody radiation significantly contributes to energy dissipation (as indicated by the vertical contours in the figure). Furthermore, in this regime the final temperature is independent of the sphere size (provided that $r \ll \lambda$), since both the optical absorption and blackbody radiation scale linearly with volume. For losses of $\sim$10 dB/km, one finds that over 10 W/μm^2 of power can be sustained without exceeding the melting point of a typical material.

Derivation of optomechanical coupling strength. Generally, introducing a dielectric material into an optical cavity causes the bare resonant frequency ω of a cavity mode to shift by an amount $\delta\omega$, which in perturbation theory is given by (4)

$$\frac{\delta\omega}{\omega} = -\frac{1}{2}\frac{\int d^3\mathbf{r}\delta P(\mathbf{r})\cdot\mathbf{E}(\mathbf{r})}{\int d^3\mathbf{r}\epsilon_0\mathbf{E}^2(\mathbf{r})}. \qquad \textbf{[S6]}$$

Here $\mathbf{E}(\mathbf{r})$ is the bare cavity mode profile and $\delta P(\mathbf{r})$ is the variation in permittivity introduced by the dielectric object. Considering the case where the dielectric object is a sub-wavelength sphere, its dielectric response is well-approximated by a point dipole, $P(\mathbf{r}') \approx \alpha_{\rm ind}E(\mathbf{r})\delta(\mathbf{r}-\mathbf{r}')$, where $\mathbf{r}$ is the center-of-mass (CM) position of the sphere. Taking a mode profile $E \propto \cos(kx-\phi)$, one readily finds (up to a constant shift) that

$$\delta\omega = -\frac{3V}{4V_c}\frac{\epsilon-1}{\epsilon+2}\cos(2kx-2\phi)\omega. \qquad \textbf{[S7]}$$

The interaction Hamiltonian between this optical mode and the mechanical motion is subsequently given by $H_{\rm om} = \hbar\delta\omega\hat{a}^\dagger\hat{a}$, and as in the main text, one can define a characteristic optomechanical coupling strength $g = \frac{3V}{4V_c}\frac{\epsilon-1}{\epsilon+2}\omega$.

Optical self-cooling equations. Here we derive in detail the cooling rate equations for the CM motion of the sphere, whose results are summarized in the main text. We begin with the Hamiltonian given by Eq. **4** in the main text. The corresponding Heisenberg equations of motion, including dissipation, are

$$\begin{aligned}
\frac{d}{dt}\hat{a}_1 &= (i\delta_1 - \kappa/2)\hat{a}_1 - \frac{i\Omega}{2} + \sqrt{\kappa}\hat{a}_{1,\rm in},\\
\frac{d}{dt}\hat{a}_2 &= (i(\delta_2 + 2gk\hat{z}) - \kappa/2)\hat{a}_2 - \frac{i\Omega}{2}\sqrt{2\zeta'} + \sqrt{\kappa}\hat{a}_{2,\rm in},\\
\frac{d}{dt}\hat{p} &= -4\hbar gk^2\hat{a}_1^\dagger\hat{a}_1\hat{z} + 2\hbar gk\hat{a}_2^\dagger\hat{a}_2 - \gamma\hat{p}/2 + \hat{F}_p(t),\\
\frac{d}{dt}\hat{x} &= \frac{\hat{p}}{m}.
\end{aligned} \qquad \textbf{[S8]}$$

Here $\hat{a}_{\rm i,in}$ are input-field operators associated with the cavity mode losses κ, γ is the damping rate of the motion, and $\hat{F}_p$ is the noise force acting on the sphere. In the above equations, we have expanded the position-dependent opto-mechanical coupling terms $g_i\cos 2(k_i\hat{x}-\phi_i)$ to first order in the displacement $\hat{x}$, and for simplicity have assumed that the two cavity modes have similar properties ($g_1 \approx g_2 = g$, etc.). We now apply shifts to all of the operators, $\hat{a}_{\rm i} \to \hat{a}_{\rm i} + \alpha_i, \hat{x} \to \hat{x} + x_0$, where the constants x_0 and α_i are chosen to cancel out all of the constant terms in the equations of motion. This yields

$$\alpha_1 = -\frac{i\Omega}{\kappa}, \qquad \textbf{[S9]}$$

$$\alpha_2 = -\frac{i\Omega}{2}\frac{\sqrt{2\zeta'}}{(\kappa/2) - i\delta_2'}, \qquad \textbf{[S10]}$$

where $\delta_2' = \delta_2 + 2gkx_0$ is the detuning relative to the new resonance frequency of the cavity when the sphere sits at $x = x_0$ rather than $x = 0$. Physically, $x = x_0$ corresponds to the minimum of the total optical potential formed by the two driven cavity modes. We define the ratio of the cavity mode intensities to be $2\zeta \equiv |\alpha_2/\alpha_1|^2$, which is equivalent to $\zeta = \zeta'\kappa^2/(\kappa^2 + 4\delta_2'^2)$. In terms of ζ, the shifted equilibrium position is given by $kx_0 = \zeta$. Clearly then the expansion in $\hat{x}$ of the opto-mechanical coupling terms requires that ζ be small. For simplicity, the prime symbol in δ_2' will be implicitly understood, and we also take $\delta_1 = 0$ in the following discussions. Following the shifts to the operators $\hat{a}_{\rm i}$ and $\hat{x}$ and then linearizing the equations of motion, one finds

$$\begin{aligned}
\frac{d}{dt}\hat{a}_1 &= -4igk^2x_0\alpha_1\hat{x} - (\kappa/2)\hat{a}_1 + \sqrt{\kappa}\hat{a}_{1,\rm in},\\
\frac{d}{dt}\hat{a}_2 &= (i\delta_2 - \kappa/2)\hat{a}_2 + 2ig\alpha_2 k\hat{x} + \sqrt{\kappa}\hat{a}_{2,\rm in},\\
\frac{d}{dt}\hat{p} &= -4\hbar gk^2|\alpha_1|^2\hat{x} + -\gamma\hat{p}/2 + \hat{F}_p(t)\\
&\qquad + 2\hbar gk(\alpha_2\hat{a}_2^\dagger + \alpha_2^*\hat{a}_2 - 2kx_0(\alpha_1\hat{a}_1^\dagger + \alpha_1^*\hat{a}_1)),\\
\frac{d}{dt}\hat{x} &= \hat{p}/m.
\end{aligned} \qquad \textbf{[S11]}$$

Note that cavity mode 1 provides a linear restoring force $d\hat{p}/dt \sim -4\hbar gk^2|\alpha_1|^2\hat{x} = -m\omega_m^2\hat{x}$, and it is straightforward to show that this relation leads to the expression for the harmonic oscillator frequency ω_m given in Eq. **1** of the main text. Furthermore, note that the sphere is opto-mechanically coupled to mode 1 with an amplitude $4gk^2x_0\alpha_1 \propto \zeta$, and to mode 2 with an amplitude $2gk\alpha_2 \propto \sqrt{\zeta}$. Thus, to lowest order in ζ, modes 1 and 2 are purely responsible for optical trapping and cooling, respectively. Treating mode 1 simply as an external harmonic potential for the sphere, the opto-mechanical system comprised of the CM motion of the sphere and cavity mode 2 is completely equivalent to the system described in ref. 5. In particular, the optical self-heating and self-cooling rates $R_\pm$ given in the main text follow immediately. For convenience, we also redefine the phases of the operators to make the optomechanical driving amplitude $\Omega_m = 2\hbar gk\alpha_2 = 2\hbar gk\alpha_1\sqrt{2\zeta}$ real.

Noise forces acting on trapped sphere. In the main text, we have derived the motional heating rates of the sphere due to background gas collisions and photon recoil kicks, which under realistic conditions are the dominant heating mechanisms. Here, we derive the heating rates for a number of other less important processes.

Photon shot noise.
Photon shot noise inside the cavity leads to heating via fluctuations in the mechanical oscillator frequency ω_m. We write the varying mechanical frequency in the form

$$\omega_m^2(t) = \omega_{m,0}^2\left(1 + \frac{\delta N(t)}{N_0}\right), \qquad \text{[S12]}$$

where $\omega_{m,0}, N_0$ are the mean frequency and mean photon number in the trapping mode of the cavity, and δN is the number fluctuation of this mode. Following the techniques of ref. 6, the shot noise leads to parametric transitions (where the phonon number $n \to n \pm 2$ jumps in pairs) at a rate R proportional to the power spectral density of the fluctuations at frequency $2\omega_{m,0}$,

$$R_{n\to n+2} = \frac{\pi\omega_{m,0}^2}{16} S(2\omega_{m,0})(n+2)(n+1), \qquad \text{[S13]}$$

$$R_{n\to n-2} = \frac{\pi\omega_{m,0}^2}{16} S(2\omega_{m,0}) n(n-1). \qquad \text{[S14]}$$

Here the power spectral density is defined by

$$S(\omega) = \frac{2}{\pi N_0^2}\int_0^\infty dt \cos\omega t \langle \delta \mathrm{N}(t)\delta N(0)\rangle, \qquad \text{[S15]}$$

which is evaluated to be $S(\omega) = \frac{1}{\pi N_0}\frac{4\kappa}{\kappa^2+4\omega^2}$ for a cavity of linewidth κ driven on resonance. Assuming that the sphere initially is in the ground state, the number of oscillations before a quantum jump due to shot noise is

$$N_{\mathrm{osc}}^{(\mathrm{sn})} = \frac{\omega_{m,0}}{2\pi R_{0\to 2}} = \frac{\epsilon+2}{\epsilon-1}\frac{V_c\rho}{3\pi c\hbar k^3}\frac{\omega_{m,0}}{\kappa}(\kappa^2 + 16\omega_{m,0}^2). \qquad \text{[S16]}$$

Here, $k = 2\pi/\lambda$ is the wavevector of the trapping beam and V_c is the cavity mode volume. As an example, we consider a cavity of length $L = 1$ cm and waist $w = 25\mu$m ($V_c = (\pi/4)Lw^2$), and a sphere of permittivity $\epsilon = 2$, density $\rho = 2$ g/cm^3, $\lambda = 1$ μm, and trapping frequency $\omega_m/(2\pi) = 0.5$ MHz (the same parameters as in Table 1 of the main text). $N_{\mathrm{osc}}^{(\mathrm{sn})}$ as a function of cavity finesse $\mathscr{F}$ ($\mathscr{F} = \pi c/\kappa L$) is plotted in Fig. S3. It can be seen that the number of allowed oscillations is at least of order $N_{\mathrm{osc}}^{(\mathrm{sn})} \sim 10^{10}$, which is much larger than the limit due to photon recoil. Physically, the low heating rates are attributable to the large intra-cavity intensities used to achieve $\sim$ MHz mechanical oscillation frequencies, which suppresses the fractional noise $\delta N/N_0 \propto N_0^{-1/2}$.

Blackbody radiation.
As in the case of scattering of laser light, the absorption and emission of blackbody radiation by the sphere also lead to recoil heating. The absorption rate of blackbody radiation of mode $\mathbf{k}$ is given in Eq. **S4** (with each absorption event providing a momentum kick $\hbar k_x$ along the trapping axis), and again we assume that $\epsilon(\omega) \approx \epsilon_{bb}$ is approximately flat across the blackbody radiation spectrum. Summing over all modes, the characteristic jump rate due to absorption of blackbody radiation is then given by (cf. Eq. **2** in main text)

$$\gamma_{\mathrm{bb}} = \frac{2\pi^4}{63}\frac{(k_B T)^6}{c^5\hbar^5\rho\omega_m}\mathrm{Im}\frac{\epsilon_{\mathrm{bb}}-1}{\epsilon_{\mathrm{bb}}+2}. \qquad \text{[S17]}$$

The jump rate between harmonic oscillator levels is $R_{n\to n\pm1} = \gamma_{\mathrm{bb}}(n + 1/2 \pm 1/2)$. An analogous expression holds for heating via the emission of blackbody radiation, with the replacement $T \to T_{\mathrm{int}}$. Note that γ_{bb} is size-independent for small spheres, as both the absorption rate and mass scale linearly with V. Using the system parameters in Table 1 of the main text, where the background temperature is $T \sim 300$ K and laser absorption leads to an internal temperature of $T_{\mathrm{int}} \sim 380$ K, we find that the number of oscillations before a quantum jump (due to either absorption or emission) is $N_{\mathrm{osc}}^{(\mathrm{bb})} \sim 10^{10}$.

Anisotropy of sphere.
The general problem of the rotational motion of an arbitrary dielectric object inside an optical cavity is quite challenging to solve. Generally, the polarizability α_{ind} becomes a function of its orientation, and changes in its orientation lead to changes in the optical trapping potential and the intra-cavity intensity. Here we consider a simplified version of the problem, where the rotational motion is limited to one axis, and the anisotropy or deformation of the sphere is of spheroid-type. As in the case of the sphere, the latter assumption admits analytical solutions for the polarizability tensor of the object (7). In particular, we assume that the dielectric is a prolate nanospheroid whose size is much smaller than the optical wavelength, with semi-major axis a and semi-minor axis b, and that the ratio $a/b \approx 1$ (i.e., the deviation from an ideal sphere is small). Then the polarizability of the spheroid is given by

$$\alpha_{\mathrm{ind}} \approx \alpha_{\mathrm{ind},0}\left(1 \pm \frac{9}{20}\frac{\epsilon-1}{\epsilon+2}[(a/b)^{4/3}-1]\right) \qquad \text{[S18]}$$

with $\alpha_{\mathrm{ind},0} \approx 3\epsilon_0 V\frac{\epsilon-1}{\epsilon+2}$. Here, the $\pm$ symbols denote when the major and minor axes are aligned along the field polarization axis, respectively. From Eqs. **S6** and **S18**, it is straightforward to find the shift in the cavity frequency taking into account the rotational degree of freedom,

$$\delta\omega = \delta\omega_0 + \delta\omega_\theta \cos 2\theta, \qquad \text{[S19]}$$

where $\delta\omega_0$ is the shift associated with the CM position alone (as given by Eq. **S7**), and

$$\delta\omega_\theta = \frac{27}{80}\frac{V}{V_c}\left(\frac{\epsilon-1}{\epsilon+2}\right)^2[(a/b)^{4/3}-1]\omega\cos(2kx - 2\phi). \qquad \text{[S20]}$$

Here, we have defined θ as the angle of rotation of the spheroid.

We are now interested in deriving the effect of the rotational motion on the CM motion. In analogy with Eq. **S8**, the coupled equations of motion between the rotation and the trapping mode are

$$\begin{aligned}\frac{da_1}{dt} &= -(i\delta\omega_\theta\cos 2\theta + \frac{\kappa}{2})a_1 + \frac{i\Omega}{2},\\ \frac{dp_\theta}{dt} &= 2\hbar\delta\omega_\theta|a_1|^2\sin 2\theta - \gamma_\theta p_\theta + F_\theta(t),\\ \frac{d\theta}{dt} &= \frac{p_\theta}{I_\theta},\end{aligned} \qquad \text{[S21]}$$

where p_θ is the angular momentum associated with θ, I_θ is the moment of inertia, and γ_θ, F_θ are the damping coefficient and noise force acting on the rotational motion. Since the rotational energy is of order $\sim k_B T$, it suffices to consider the classical equations given here. The damping term is effected through the background gas, as each collision between the spheroid and a gas molecule partly exchanges angular momentum between the two systems. The damping coefficient is found to be $\gamma_\theta = 5\sqrt{3/(2\pi)}\alpha_\theta P/(v_{\mathrm{rms}} r\rho)$ (8), where $r \approx a \approx b$. α_θ is a phenomenological accommodation coefficient describing the efficiency of angular momentum transfer. The noise force has correlations $\langle \mathrm{F(t)F(t')}\rangle = 2D\delta(t-t')$, where $D = \gamma_\theta k_B T/I_\theta$. Note that γ_θ is a very small quantity under good vacuum conditions.

The full nonlinear coupled equations of Eq. **S21** are difficult to treat in a general setting. However, given the typical smallness of the parameters $\delta\omega_\theta/\kappa$ and $\hbar\delta\omega_\theta|a_1|^2/(k_BT)$ for nearly spherical particles, to lowest order we can ignore the optical coupling to the rotational motion, and the dominant effect of the sphere anisotropy is trap heating through fluctuations in the polarizability $\alpha_{\rm ind}$ rather than intra-cavity intensity fluctuations. This leads to fluctuations in the trap frequency given by

$$\delta\omega_m(t) = \epsilon_\theta \omega_{m,0} \cos 2\theta(t), \qquad \textbf{[S22]}$$

where $\epsilon_\theta = \frac{9}{40}\frac{\epsilon-1}{\epsilon+2}((a/b)^{4/3}-1)$. As in the case of shot noise, these fluctuations in the mechanical frequency lead to parametric heating, with a jump rate out of the ground state given by

$$R_{0\to 2} = \int_0^\infty dt \cos 2\omega_{m,0} t \langle \delta\omega_{\rm m}(0)\delta\omega_{\rm m}(t)\rangle. \qquad \textbf{[S23]}$$

Denoting $\delta\theta(t) = \theta(t) - \theta(0)$, the above equation can be rewritten in the form

$$R_{0\to 2} = \frac{1}{2}\int_0^\infty dt \cos 2\omega_{m,0} t (\epsilon_\theta \omega_{m,0}^2)^2 \langle \cos 2\delta\theta(t)\rangle. \qquad \textbf{[S24]}$$

Making a Gaussian approximation $\langle e^{2i\delta\theta(t)}\rangle \approx \exp(-\langle\delta\theta^2(t)\rangle/2)$, and taking the limit of small γ_θ, one finally finds

$$\frac{R_{0\to 2}}{\omega_{m,0}} = \epsilon_\theta^2 \frac{\sqrt{2\pi}\omega_{m,0}}{8\sqrt{\langle\omega_{\rm r}^2\rangle}} \exp\left(-\frac{\omega_{m,0}^2}{2\langle\omega_{\rm r}^2\rangle}\right). \qquad \textbf{[S25]}$$

Here, $\omega_r = d\theta/dt$ is the angular velocity of the spheroid (typical values of $\sqrt{\langle\omega_{\rm r}^2\rangle}$ are in the MHz range for sub-wavelength particles). Note that the above function is peaked at $\omega_{m,0} = \sqrt{\langle\omega_{\rm r}^2\rangle}$, i.e., the parametric heating is most pronounced when the rotational frequency is comparable to the CM oscillation frequency. At this maximum, $R_{0\to 2}/\omega_{m,0} \sim 0.2\epsilon_\theta^2$. Furthermore, for this worst-case scenario, $R_{0\to 2}/\omega_{m,0}$ can be suppressed to the $\sim 10^{-5}$ level with an anisotropy of $a/b \sim 1.1$.

Analysis of entanglement transfer. Here we provide a detailed analysis of entanglement transfer between two modes of light and two spatially separate spheres, leading to Eq. **8** in the main text. The EPR correlations between the two light modes given by Eq. **7** in the main text,

$$\left\langle \left(X^{(\rm A)}_{\pm,\rm in}(\omega) \pm X^{(B)}_{\pm,\rm in}(\omega)\right)^2 \right\rangle/2 = e^{-2R} < 1, \qquad \textbf{[S26]}$$

are of the form created by a non-degenerate optical parametic amplifier (NOPA) (9), which we describe below.

The Hamiltonian corresponding to a NOPA with cavity modes A,B is given by

$$H = i\hbar(\beta/2)(\hat{c}^{(A)}\hat{c}^{(B)} - \hat{c}^{(A)\dagger}\hat{c}^{(B)\dagger}), \qquad \textbf{[S27]}$$

where $\hat{c}^{(j)}$ is the annihilation operator of mode j. Taking an ideal, one-sided cavity (10), and assuming that the modes have identical linewidths κ_c, the Heisenberg equations of motion for each mode read

$$\frac{d}{dt}\hat{c}^{(j)} = -\frac{\kappa_c}{2}\hat{c}^{(j)} - \frac{\beta}{2}\hat{c}^{(j')\dagger} + \sqrt{\kappa_c}\hat{c}^{(j)}_{\rm in}. \qquad \textbf{[S28]}$$

Here $\hat{c}^{(j)}_{\rm in}$ is the cavity input field for mode j, and $j' = A,B$ for $j = B,A$. The output field is related to the intracavity and input fields by $\hat{c}^{(j)}_{\rm out} = \sqrt{\kappa_c}\hat{c}^{(j)} - \hat{c}^{(j)}_{\rm in}$. Writing $\hat{c}^{(j)}(t) = (1/\sqrt{2\pi})\int d\omega e^{-i\omega t}\hat{c}^{(j)}(\omega)$, Eq. **S28** can be exactly solved in the Fourier domain for $\hat{c}^{(j)}(\omega)$. Specifically, defining quadrature operators $\hat{X}^{(j)}_+ = \hat{c}^{(j)} + \hat{c}^{(j)\dagger}$ and $\hat{X}^{(j)}_- = (\hat{c}^{(j)} - \hat{c}^{(j)\dagger})/i$ (with analogous definitions for the quadrature operators of the input and output fields), one can show when $\beta < \kappa_c$ that

$$\hat{X}^{(A)}_{\pm,\rm out}(\omega) \pm \hat{X}^{(B)}_{\pm,\rm out}(\omega) = \frac{\kappa_c - \beta + 2i\omega}{\kappa_c + \beta - 2i\omega}\left(\hat{X}^{(A)}_{\pm,\rm in}(\omega) \pm \hat{X}^{(B)}_{\pm,\rm in}(\omega)\right). \qquad \textbf{[S29]}$$

Over a bandwidth $\Delta\omega \ll \kappa_c$ that is much smaller than the cavity linewidth, one can ignore the ω dependence in the equation above, yielding

$$\hat{X}^{(A)}_{\pm,\rm out}(\omega) \pm \hat{X}^{(B)}_{\pm,\rm out}(\omega) = e^{-R}\left(\hat{X}^{(A)}_{\pm,\rm in}(\omega) \pm \hat{X}^{(B)}_{\pm,\rm in}(\omega)\right), \qquad \textbf{[S30]}$$

where $e^{-R} = \frac{\kappa_c-\beta}{\kappa_c+\beta}$ for $\beta < \kappa_c$. Physically, for non-zero β, the joint variance of these quadratures in the output fields can display reduced fluctuations relative to the input fields. It can also be shown that the other combinations of the quadratures (for $\Delta\omega \ll \kappa_c$) satisfy

$$\hat{X}^{(A)}_{\pm,\rm out}(\omega) \mp \hat{X}^{(B)}_{\pm,\rm out}(\omega) = e^{R}\left(\hat{X}^{(A)}_{\pm,\rm in}(\omega) \mp \hat{X}^{(B)}_{\pm,\rm in}(\omega)\right), \qquad \textbf{[S31]}$$

such that their joint variances become enhanced. For this discussion, the input fields to the NOPA are assumed to be vacuum states.

We now consider the quantum state transfer process for two spheres trapped in spatially separate cavities, where the two output fields generated by NOPA are fed as input fields into each of the opto-mechanical systems. The equations of motion for the two opto-mechanical systems (denoted A,B) are given by Eq. **6** in the main text, with the replacement $\hat{a}^{(j)}_{2,\rm in} = \hat{c}^{(j)}_{\rm out}$. As in the main text, for simplicity we suppress the subscript "2" in the field operators denoting the cooling mode, since we are only interested in this mode from this point on. To solve these equations, we again work in the Fourier domain. Without the fast-rotating terms $e^{2i\omega_m t}$, one could achieve ideal state transfer between the mechanical motion and light, as discussed in the main text. When the fast-rotating terms $e^{2i\omega_m t}$ are included in the analysis, the frequency components $\omega, \omega + 2n\omega_m$ (integer n) of the operators are coupled together in an infinite set of algebraic equations. To make the problem tractable, we truncate this infinite set by ignoring the components $\hat{a}^{(j)}(\omega + 2n\omega_m), \hat{b}^{(j)}(\omega + 2n\omega_m)$ where $|n| \geq 2$ (*e.g.*, we assume $\hat{a}^{(j)}(\omega \pm 4\omega_m) = 0$). This truncation essentially amounts to the assumption that ω_m is large compared to the other frequency scales in the problem. We then solve the coupled set of equations for $\hat{a}^{(j)}(\omega), \hat{b}^{(j)}(\omega)$ in terms of $\hat{F}^{(j)}(\omega)$ and $\hat{a}^{(j)}_{\rm in}(\omega)$ (or $\hat{c}^{(j)}_{\rm in}(\omega)$), which allows us to obtain any correlation functions for the cavity field or mechanical motion in terms of those of the noise and input fields. The noise forces $\hat{F}^{(j)}$ are assumed to be dominated by photon recoil heating and are independent for the systems A,B, such that their correlations take the form $\langle\hat{\rm F}^{(\rm j)}(\omega)\rangle = 0$ and $\langle\hat{\rm F}^{(\rm j)}(\omega)\hat{\rm F}^{(\rm j')}(\omega')\rangle = \phi\omega_m\delta(\omega+\omega')\delta_{jj'}$, where $\phi = (4\pi^2/5)(V/\lambda^3)\frac{\epsilon-1}{\epsilon+2}$ (see main text). We are specifically interested in the quantity

$$\Delta_{\rm EPR} \equiv \left\langle \left(X^{(\rm A)}_{\pm,\rm m}(t) \mp X^{(B)}_{\pm,m}(t)\right)^2 \right\rangle/2 \qquad \textbf{[S32]}$$

characterizing the joint variance in the motion of the two spheres. The solution is generally quite complicated, but can be expanded to lowest order in the small parameter κ/ω_m (it is reasonably

assumed that sideband resolution can be achieved, so that $\kappa/\omega_m \ll 1$). After performing this procedure, and also ignoring any fast-rotating terms ($e^{\pm 2i\omega m t}$) in the final expression for Δ_{EPR}, one arrives at the solution given by Eq. **8** in the main text.

Analysis of squeezed light generation. Here we derive the squeezing amplitude given in Eq. **9** of the main text. In the main text, it was argued that the trapping mode of the cavity can be effectively considered as a mechanical potential in the limit of small ζ. We consider the situation where the trapping beam intensity is varied to produce a sinusoidal component in the mechanical spring constant at frequency $2\omega_m$, with an effective Hamiltonian for the motion given by

$$H_m = \frac{\hat{p}^2}{2m} + \frac{1}{2}m\omega_m^2\hat{x}^2(1 + 2\epsilon_m \sin 2\omega_m t) \qquad \text{[S33]}$$

$$= \hbar\omega_m \hat{\mathrm{b}}^\dagger\hat{b} - i\frac{\hbar\beta}{2}\left(\hat{b}^2 e^{2i\omega_m t} - \hat{\mathrm{b}}^{\dagger 2} e^{-2i\omega_m t}\right) + 2\left\{\hbar\beta\hat{\mathrm{b}}^\dagger\hat{b}\sin 2\omega_m t\right\}. \qquad \text{[S34]}$$

In the last line, we have re-written $\hat{x} = \sqrt{\frac{\hbar}{2m\omega_m}}(\hat{b} + \hat{\mathrm{b}}^\dagger)$ and $\hat{p} = i\sqrt{\frac{\hbar m\omega m}{2}}(\hat{\mathrm{b}}^\dagger - \hat{b})$ in terms of the harmonic oscillator annihilation operator $\hat{b}$ and also defined $\beta = \epsilon\omega_m/2$ (unrelated to the β term defined in the previous section for a NOPA). The term in braces is a fast-varying contribution to the Hamiltonian, in addition to the "ideal" squeezing Hamiltonian comprising the remaining terms. The external Hamiltonian H_e (see Eq. **6** in the main text) in this case is

$$H_e = -i\frac{\hbar\beta}{2}(\hat{b}^2 e^{2i\omega_m t} - \hat{\mathrm{b}}^{\dagger 2} e^{-2i\omega_m t}) + 2\hbar\beta\hat{\mathrm{b}}^\dagger\hat{b}\sin 2\omega_m t, \qquad \text{[S35]}$$

and the Heisenberg equations of motion read

$$\frac{d}{dt}\hat{\mathrm{a}}_2 = -\frac{\kappa}{2}\hat{\mathrm{a}}_2 - i\Omega_m(\hat{b} + \hat{\mathrm{b}}_2^\dagger e^{2i\omega_m t}) + \sqrt{\kappa}\hat{\mathrm{a}}_{2,\mathrm{in}},$$
$$\frac{d}{dt}\hat{b} = -i\Omega_m(\hat{\mathrm{a}}_2 + \hat{\mathrm{a}}_2^\dagger e^{2i\omega_m t}) + i\hat{F}(t)e^{i\omega_m t} + \beta\hat{\mathrm{b}}^\dagger - 2i\beta\hat{b}\sin 2\omega_m t. \qquad \text{[S36]}$$

We proceed to solve these equations in the Fourier domain using the same techniques described in the previous section for entanglement transfer. Specifically, we truncate terms containing frequency components $\omega + 2n\omega_m$ (integer n) at $|n| \geq 2$ and solve for $\hat{a}(\omega), \hat{b}(\omega)$ in terms of $\hat{F}(\omega)$ and $\hat{a}_{\mathrm{in}}(\omega)$, from which any correlation functions for the cavity field or mechanical motion can be obtained. The input field is assumed to be in the vacuum state. Similarly, the properties of the output field can be obtained from these solutions by using the relation $\hat{\mathrm{a}}_{\mathrm{out}} = \sqrt{\kappa}\hat{\mathrm{a}} - \hat{\mathrm{a}}_{\mathrm{in}}$.

We are specifically interested in the properties of the operator $X_{+,\mathrm{out}}(\omega = 0) = \hat{\mathrm{a}}_{\mathrm{out}}(\omega = 0) + \hat{\mathrm{a}}_{\mathrm{out}}^\dagger(\omega = 0)$. The general solutions of Eq. **S36** in the Fourier domain are quite cumbersome, so we consider the simplified limit where we set $\Gamma = \kappa$, and take the parametric driving strength to be $\beta = \frac{\Gamma}{2}(1 - \delta_t)$, where $\delta_t \ll 1$ is a small parameter that characterizes how far one operates from threshold ($\beta \to \Gamma/2$). Expanding to lowest order in κ/ω_m and δ_t and ignoring any fast-rotating terms that remain at the end of the calculation, we find the following variance,

$$\Delta X_{+,\mathrm{out}}^2(\omega = 0) \approx \frac{5}{16}\frac{\kappa^2}{\omega_m^2} + \frac{3}{32}\frac{\kappa^2}{\omega_m^2}\delta_t + \frac{2\phi\omega_m}{\kappa}(1 + \delta_t) + \frac{\delta_t^2}{4}. \qquad \text{[S37]}$$

In particular, at threshold ($\delta_t = 0$), one recovers Eq. **9** of the main text. Maximum squeezing of the variance on threshold is achieved when $\kappa = 2(2\phi/5)^{1/3}\omega_m$, in which case $(\Delta X_{+,\mathrm{out}}^2)_{\min} = (3/2)(5\phi^2/2)^{1/3}$.

Thus far, we have neglected to consider corrections due to a possibly large position uncertainty Δx for the CM motion of the sphere. Specifically, as one approaches threshold, one quadrature of motion becomes infinitely unsqueezed, producing a large Δx. At the same time, faithful quantum state transfer requires a linear opto-mechanical coupling, where $\mathcal{O}(x^2)$ shifts in the cavity cooling mode frequency can be ignored. Specifically, the Lamb-Dicke parameter $\eta \equiv k\Delta x \ll 1$ for the trapped sphere must remain small. To quantify this effect, we consider the situation where we operate away from threshold by an amount that decreases the squeezing by just 1 dB relative to $(\Delta X_{+,\mathrm{out}}^2)_{\min}$. The value of δ_t corresponding to this 1 dB increase can be obtained by solving Eq. **S37**, and plugged into the solutions of Eq. **S36** to numerically find Δx. For concreteness, here we associate Δx with the position uncertainty in the unsqueezed quadrature of motion. The corresponding Lamb-Dicke parameter as a function of sphere size is then plotted in Fig. S4 for the choice $\omega_m/(2\pi) = 0.5$ MHz, and it is seen that $\eta < 10^{-2}$ over the entire parameter regime.

Effect of transverse motion. Thus far we have considered the cooling and state manipulation of the motion of the sphere along the cavity axis. Here we derive in detail the corrections to these processes due to the transverse motion of the sphere. In particular, we find that the effects on the axial motion can be made small provided that the uncertainty in the transverse position is small compared to the beam waist, $\Delta y \ll w$.

First we consider the effect of transverse motion on the optical trapping potential. Assuming that the cavity mode profile has a Gaussian shape, $E(y) = E_0 e^{-y^2/w^2}$, it is straightforward to show that to lowest order, the transverse motion behaves as a harmonic oscillator with frequency

$$\omega_y = \sqrt{\frac{12I_0}{\rho c w^2}}\mathrm{Re}\frac{\epsilon - 1}{\epsilon + 2}. \qquad \text{[S38]}$$

Note that for typical parameters (beam waist much larger than the optical wavelength), the transverse oscillation frequency is very small compared to the axial frequency $\omega_{m,0} = \sqrt{\frac{6k^2 I_0}{\rho c}}\mathrm{Re}\frac{\epsilon-1}{\epsilon+2}$ at the beam center (Eq. **1** of main text), with $\omega_y/\omega_{m,0} = \sqrt{2}/(kw)$. Given the typically slow time scale for the transverse motion compared to the cavity linewidth, $\omega_y \ll \kappa$, one can assume that the intra-cavity intensity $I(t)$ is an instantaneous function of the transverse position $y(t)$,

$$I(y) = I_0\frac{\kappa^2}{\kappa^2 + 4\delta_1(y)^2}\exp\left(-\frac{2y^2}{w^2}\right), \qquad \text{[S39]}$$

where I_0 is the intra-cavity intensity when the sphere is positioned at the beam center. The term $\frac{\kappa^2}{\kappa^2+4\delta_1(y)^2}$ describes changes in the intra-cavity intensity due to changes in the cavity resonance frequency as a function of the sphere position (for a constant pump power). Assuming that the cavity is on resonance with the pump when $y = 0$, from Eq. **S6** one finds that the position-dependent detuning of the pump is $\delta_1(y) = -2g(e^{-2y^2/w^2} - 1)$, where g is the opto-mechanical coupling strength and the subscript 1 denotes the trapping mode. Note then that $\frac{\kappa^2}{\kappa^2+4\delta_1(y)^2}$ adds a correction to the intensity that is only of order $(y/w)^4$. On the other hand, the term $\exp\left(-\frac{2y^2}{w^2}\right)$ in Eq. **S39** describes direct changes in the local intensity experienced by the sphere as it moves in the beam profile, and induces corrections of order

$(y/w)^2$. Thus to lowest order, $I(y) \approx I_0(1-\frac{2y^2}{w^2})$. This in turn causes fluctuations in the axial frequency,

$$\omega_m(y(t)) \approx \omega_{m,0}\left(1-\frac{y^2}{w^2}\right). \quad \textbf{[S40]}$$

In analogy with Eq. **6** in the main text, one can define an annihilation operator $\hat{b}_y$ for the transverse motion, whose equation of motion in a rotating frame is given by

$$\frac{d}{dt}\hat{b}_y = -\gamma_y \hat{b}_y + i\hat{F}_y(t)e^{i\omega_y t}. \quad \textbf{[S41]}$$

Here γ_y is an effective decay rate for the transverse motion, which might be due to gas damping or some external cooling mechanism. $\hat{F}_y$ describes a noise force that leads to heating, which (as for the axial motion) is dominated by photon recoil in our regime of interest. It can readily be shown that for the dipole radiation pattern of the sphere,

$$\langle \hat{F}_y(t)\hat{F}_y(t')\rangle \approx \frac{\phi\omega_{m,0}^2}{\omega_y}\delta(t-t') \quad \textbf{[S42]}$$

in one transverse direction, while in the other transverse direction, the correlation function is reduced by a factor of 2. The relation between the annihilation operator and the transverse position is given by $y = \sqrt{\frac{\hbar}{2\rho V\omega_y}}(\hat{b}_y e^{-i\omega_y t} + \hat{b}_y^\dagger e^{i\omega_y t})$. In what follows, we are primarily concerned with the situation where the transverse motion is highly populated, $\langle \hat{n}_y\rangle \equiv \langle \hat{b}_y^\dagger \hat{b}_y\rangle \gg 1$, such that the operator nature of these variables is not important. In the case where the decay rate γ_y is negligible, the noise in Eq. **S42** leads to an increasing position uncertainty $\Delta y \approx w\sqrt{\phi\omega_r t}$ for a sphere initially localized at the bottom of the potential well.

Fluctuations in the axial frequency $\omega_m(t)$ due to the transverse motion cause parametric heating in the axial direction, in analogy to the effects of photon shot noise or sphere anisotropy. Following Eq. **S23**, the heating rate out of the axial ground state is given by

$$R_{0\to 2} = \int_0^\infty dt(\cos 2\omega_{m,0}t)\langle \delta\omega_{\rm m}(0)\delta\omega_{\rm m}(t)\rangle, \quad \textbf{[S43]}$$

where $\delta\omega_m = \omega_m(t) - \langle\omega_{\rm m}(t)\rangle$. By integrating Eq. **S41**, substituting into Eq. **S40** and simplifying, one finds that the heating rate due to transverse motion is

$$R_{0\to 2} \approx \frac{1}{2}\phi\omega_r\frac{\langle y^2\rangle}{w^2}. \quad \textbf{[S44]}$$

Using the parameters from Table 1 of the main text, $\phi\omega_r/2 \sim 10^{-6}$, and thus the heating caused by fluctuations in $\omega_m(t)$ can be considered negligible. Physically, this heating mechanism is small because the axial frequency tends to fluctuate at rates $\sim\omega_y$ that are much slower.

We now derive the decrease in cooling efficiency of the axial motion due to the transverse motion. There are two separate effects to consider. First, like in the case of the trapping beam, the intensity of the cooling beam changes as the sphere moves around, which affects the opto-mechanical driving amplitude Ω_m. Second, in the sideband resolved regime, the cooling mode should ideally be driven on the red motional sideband ($\delta_2 = -\omega_{m,0}$), whereas the fluctuating axial frequency ω_m and cooling mode resonance frequency cause the detuning from this sideband to drift. We first consider the fluctuations in the cooling beam intensity. Using Eq. **S6**, one finds that the transverse motion shifts the cooling mode frequency by an amount $2gy^2/w^2$ to lowest order, which causes the detuning to vary as $\delta_2 = -\omega_{m,0} - 2gy^2/w^2$. The opto-mechanical driving amplitude then varies as (cf. Eq. **S39**)

$$\Omega_m^2(y) = \Omega_{m,0}^2\frac{\kappa^2}{\kappa^2+4\delta_2(y)^2}\exp\left(-\frac{2y^2}{w^2}\right) \quad \textbf{[45]}$$

$$\approx \Omega_{m,0}^2\left(1-\frac{2y^2}{w^2}-\frac{16g\omega_{m,0}}{\kappa^2+4\omega_{m,0}^2}\frac{y^2}{w^2}\right). \quad \textbf{[46]}$$

Here we have expanded to lowest order in y and $\Omega_{m,0}$ denotes the peak amplitude at $y = 0$. We now substitute these expressions into the equation for the optical cooling and heating rates,

$$R_{\rm opt,\mp} = \frac{\kappa\Omega_m^2(y)}{(\kappa/2)^2+(\delta_2(y)\pm\omega m(y))^2}. \quad \textbf{[47]}$$

After some simplification, the average rates are given in terms of the rates at $y = 0$ ($R_{\rm opt,\mp}^{(0)}$) by

$$R_{\rm opt,+} \approx R_{\rm opt,+}^{(0)}\left(1-\frac{\langle y^2\rangle}{w^2}\left(\frac{16g\omega_{m,0}}{\kappa^2+4\omega_{m,0}^2}+\frac{\kappa^2+32g\omega_{m,0}}{\kappa^2+16\omega_{m,0}^2}\right)\right),$$
$$R_{\rm opt,-} \approx R_{\rm opt,-}^{(0)}\left(1-\frac{\langle y^2\rangle}{w^2}\left(1+\frac{16g\omega_{m,0}}{\kappa^2+4\omega_{m,0}^2}\right)\right). \quad \textbf{[48]}$$

Thus, one concludes that the decrease in cooling efficiency scales like $\sim\langle y^2\rangle/w^2$.

We now consider the limitations imposed on squeezed light generation by transverse motion. We assume that the strength and frequency of the parametric driving term are fixed, with the corresponding external Hamiltonian $H_e = m\omega_{m,0}^2\hat{x}^2\epsilon_m \sin 2\omega_{m,0}t$. Ideal squeezing occurs when the parametric driving frequency is identical to twice the axial frequency, $2\omega_{m,0} = 2\omega_m(y(t))$. However, the main effect of fluctuations is to cause the two quantities to become out of sync, which can be captured in Eq. S36 by including a time-dependent detuning,

$$\frac{d}{dt}\hat{b} = i\delta\omega_m(t)\hat{b} - i\Omega_m(\hat{a}_2+\hat{a}_2^\dagger e^{2i\omega_m t}) + i\hat{F}(t)e^{i\omega_m t} + \beta\hat{b}^\dagger - 2i\beta\hat{b}\sin 2\omega_m t. \quad \textbf{[49]}$$

Note that the opto-mechanical system tends toward a steady state in a time $\sim 1/\kappa$ that is typically much shorter than the time scale of fluctuations in ω_m. As a result, we can effectively treat the time-dependent detuning as a quasi-static quantity, solving this equation in the Fourier domain at each moment in time. For simplicity, here we ignore the non-secular terms and the noise force, as we are interested primarily in the fundamental limit on squeezing imposed by the detuning term. Applying the same methods as those used to arrive at Eq. **S37**, we find that

$$\Delta X_{+,\rm out}^2(\omega=0) \approx \left(\frac{\Gamma-2\beta}{\Gamma+2\beta}\right)^2 + \frac{32\beta\Gamma(3\Gamma-2\beta)\delta\omega_m(t)^2}{(\Gamma-2\beta)^2(2\beta+\Gamma)^2}. \quad \textbf{[50]}$$

As before, we have defined $\Gamma = 4\Omega_m^2/\kappa$ as the cavity-induced mechanical dissipation rate. For a given uncertainty in $\langle\delta\omega_{\rm m}(t)^2\rangle$, there exists an ideal value of β that minimizes the variance in $\Delta X_{+,\rm out}^2$, which is found to be $\beta \approx (1/2)(\Gamma - 2\sqrt{\Gamma\sqrt{\langle\delta\omega_{\rm m}(t)^2\rangle}})$. In this case,

$$(\Delta X_{+,\rm out}^2)_{\rm min} \approx 2\frac{\omega_{m,0}}{\Gamma}\frac{\langle y^2\rangle}{w^2}. \quad \textbf{[51]}$$

An analogous result holds for the minimum EPR variance achievable through quantum state transfer between two spheres, since the EPR state can be viewed as a two-mode squeezed state.

Finally, we estimate the effect of axial heating through nonlinear coupling between the axial and transverse motions. Specifically, the harmonic oscillator approximation is valid only close to the minimum of the potential well. More generally, the full potential is given by $U(\mathbf{r}) \approx U_0 \cos^2 kxe^{-2y^2/w^2}$, where $U_0 = \frac{3I_0V}{c}$ Re $\frac{\epsilon-1}{\epsilon+2}$ as given in the main text. For simplicity, here we ignore any position dependence in the optical force that is induced through a shift in the cavity resonance frequency and thus the intra-cavity intensity. Note that the above potential contains a nonlinear cross-coupling term between the axial and transverse motions, which at lowest order is given by $U_{\text{an}} \approx 2U_0(y/w)^2(kx)^2$. This coupling can induce transitions between phonon numbers $n_x, n_y \to n_x + 2, n_y - 2$. Averaging over the transverse position, the corresponding transition rate $R(n_x)$ is given by

$$R(n_x) \sim \frac{\Gamma}{36}(n_x+1)(n_x+2)^2\left(\frac{\langle y^2\rangle}{w^2}\right)^2. \quad [52]$$

Note that this nonlinear mixing enables weak cooling of the transverse motion through cooling of the axial motion, but this is typically insignificant compared to the transverse recoil heating rate. In addition, under good vacuum conditions (say at $P = 10^{-10}$ Torr), the maximum energy damping due to the background gas is also an order of magnitude smaller than the heating rate, using the parameters in Table 1 in the main text. Thus, at least some weak, external cooling mechanism must be occasionally applied in order to position the sphere near the center of the beam waist. Once initialized, however, the uncertainty due to recoil heating grows very slowly in time, $\Delta y \approx w\sqrt{\phi\omega_r t}$, as thousands of seconds are required before $(\Delta y/w)^2 \sim 0.01$.

1. Stratton JA (1941) Electromagnetic Theory, 1st Ed, McGraw-Hill, New York.
2. Liu F, Daun KJ, Snelling DR, and Smallwood GJ (2006) Heat conduction from a spherical nano-particle: status of modeling heat conduction in laser-induced incandescence. *Appl Phys B* 83:355–382.
3. Lang ML and Wolfe WL (1983) Optical constants of fused silica and sapphire from 0.3 to 25 μm. *Appl Opt* 22:1267–1268.
4. Rodriguez A, Soljacic M, Joannopoulos JD, and Johnson SG (2007) $\chi^{(2)}$ and $\chi^{(3)}$ harmonic generation at a critical power in inhomogeneous doubly resonant cavities. *Opt Express* 15:7303–7318.
5. Wilson-Rae I, Nooshi N, Zwerger W, and Kippenberg TJ (2007) Theory of ground state cooling of a mechanical oscillator using dynamical backaction. *Phys Rev Lett* 99:093901.
6. Gehm ME, O'Hara KM, Savard TA, and Thomas JE (1998) Dynamics of noise-induced heating in atom traps. *Phys Rev A* 58:3914–3921.
7. Klimov VV, Ducloy M, Letokhov VS (2002) Spontaneous emission of an atom placed near a prolate nanospheroid. *Eur Phys J D* 20:133–148.
8. Volkov AN (2009) Aerodynamic coefficients of a spinning sphere in a rarefied-gas flow. *Fluid Dyn* 44:141–157.
9. Ou ZY, Pereira SF, Kimble HJ, and Peng KC (1992) Realization of the Einstein–Podolsky–Rosen paradox for continuous variables. *Phys Rev Lett* 68:3663–3666.
10. Gardiner CW, Collett MJ (1985) Input and output in damped quantum systems: Quantum stochastic differential equations and the master equation. *Phys Rev A* 31:3761–3774.

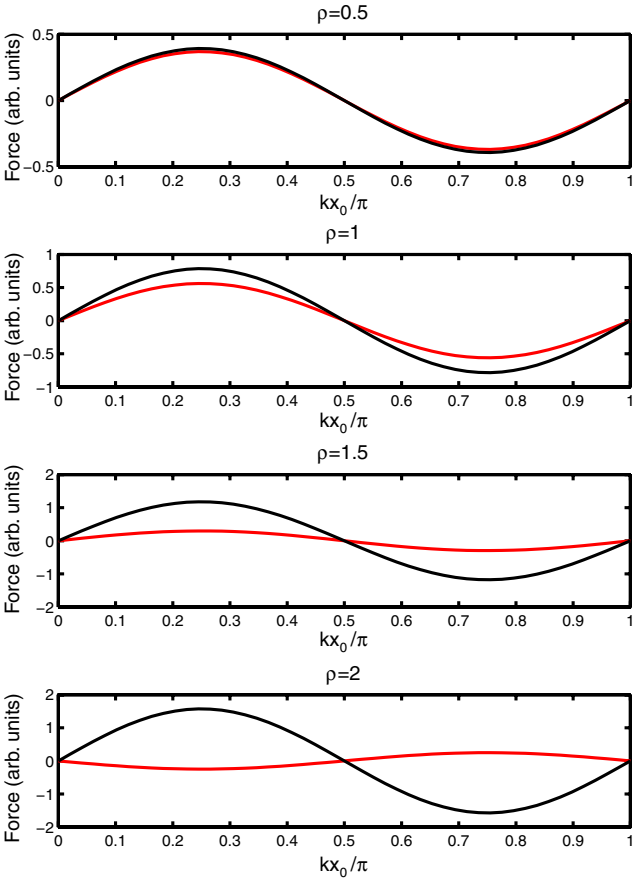

Fig. S1. Comparison of optical forces (in arbitrary units) acting on a dielectric sphere of permittivity $\epsilon = 2$ as a function of position kx_0. The four figures shown correspond to sphere sizes of $\rho \equiv k\sqrt{\epsilon}r = 0.5$, 1, 1.5, 2. The black curve indicates the results obtained from an electrostatic, point-dipole approximation, while the red curve denotes exact electrodynamical theory.

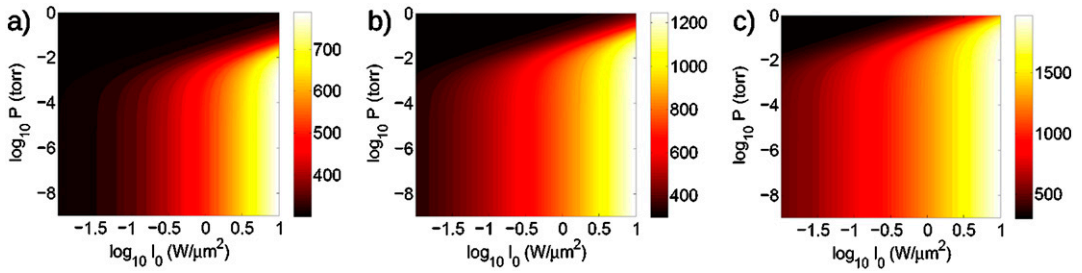

Fig. S2. Internal temperature of sphere (in K), as functions of background gas pressure and intra-cavity intensity. Material parameters for the sphere are given in the text. Optical losses for the sphere are assumed to be (a) 10, (b) 100, and (c) 1,000 dB/km.

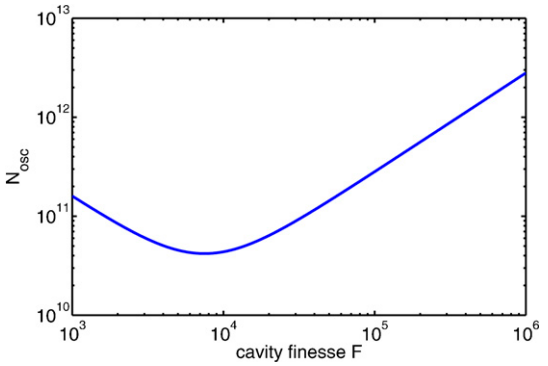

Fig. S3. The number of coherent oscillations N_{osc} allowed before a quantum jump due to shot noise, as a function of cavity finesse. The system parameters are given in the text.

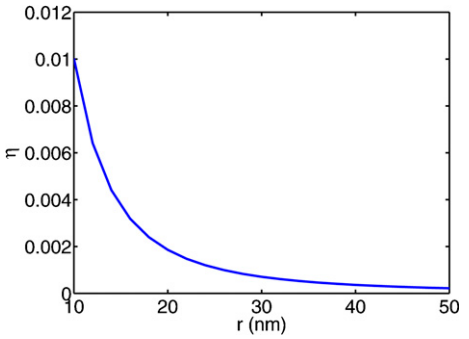

Fig. S4. The Lamb–Dicke parameter $\eta = k\Delta x$ corresponding to the squeezed motional state of the sphere, as a function of sphere size. The squeezing parameters are chosen such that the squeezing in the output light is increased by 1 dB over $(\Delta X^2_{+,\mathrm{out}})_{\mathrm{min}}$. The physical parameters of the system are taken to be $\lambda = 1\mu$m, $\rho = 2$ g/cm^3, $\epsilon = 2$, and $\omega_m/2\pi = 0.5$ MHz.